Journal of Magnetism and Magnetic Materials 496 (2020) 165912

Contents lists available at ScienceDirect

Journal of Magnetism and Magnetic Materials

journal homepage: www.elsevier.com/locate/jmmm

Research articles

A ferromagnetic skyrmion-based nano-oscillator with modified profile of Dzyaloshinskii-Moriya interaction

J.H. Guo[a], J. Xia[b], X.C. Zhang[b], Philip W.T. Pong[a,*], Y.M. Wu[c], H. Chen[d], W.S. Zhao[e], Y. Zhou[b,*]

[a] Department of Electrical and Electronic Engineering, The University of Hong Kong, Hong Kong, China
[b] School of Science and Engineering, The Chinese University of Hong Kong, Shenzhen, Guangdong 518172, China
[c] School of Information Science and Technology, Fudan University, Shanghai 200433, China
[d] School of Materials Science and Energy Engineering, Foshan University, Guangdong 528000, China
[e] Fert Beijing Institute, BDBC, School of Microelectronics, Beihang University, Beijing, China

ARTICLE INFO

Keywords:
Magnetic skyrmions
Spin torque nano-oscillators
Dzyaloshinskii-Moriya interactions
Spintronics
Micromagnetics

ABSTRACT

Magnetic skyrmions have attracted great interest in recent years due to their potential wide-scale applications in spintronic devices, such as the spin torque nano-oscillator (STNO) and racetrack memory. The spin-transfer torque can drive the motion of skyrmions on a ferromagnetic nanodisk, where skyrmions are stabilized by the Dzyaloshinskii-Moriya interaction (DMI). However, the Magnus force acted on a skyrmion can drive the skyrmion moving toward either the nanodisk center or edge, which may lead to the destruction of skyrmion at edge, and thus reduce the performance of skyrmion-based STNO. In order to overcome this problem, we designed a ferromagnet/spacer/ferromagnet/heavy metal STNO model, in which the inner and outer areas of the ferromagnetic nanodisk have different DMI, and those skyrmions could move along the boundary between inner and outer areas. We investigated the dynamics of skyrmions in such a STNO model by adjusting several geometrical and material parameters. We obtained an optimal frequency of skyrmion oscillation of 3.43 GHz. Our results may be useful for designing future STNOs based on skyrmions, where the Magnus-force-induced destruction of skyrmions can be effectively avoided.

1. Introduction

With the rapid development of advanced technologies such as big data analysis and artificial intelligence [1–3], the demand for better information storage and processing equipment has also been increased [4,5]. Magnetic skyrmions have been widely considered to be used in next-generation spintronic devices because of their rigid shape [6,7], small size [8–10], reasonable stability [11,12], and the creation of lower Joule heating in metallic materials due to their small depinning and driving current density [9,13–16]. Electric current is basically formed by the directional motion of free electrons. Electrons' spin directions are randomly distributed, and the whole of the nucleus is neutral, i.e. without polarity. When a vertical current is injected into a ferromagnet/non-ferromagnet bilayer structure spin valve, the spin scattering occurs, which in turn, generates spin current and spin-transfer torque (STT) [4,17,18]. Magnetic skyrmions can be used for building different information devices driven by STT, such as the racetrack memory [11,19,20] and spin torque nano-oscillator (STNO) [1,4,12,18,21]. Compared with magnetic vortex-based STNO [21], skyrmion-based STNO could demonstrate a higher and steadier maximum working frequency [22–24] and broader tenability [25,26].

Magnetic skyrmions were first observed in bulk non-centrosymmetric B20-type transition metal compounds and were then detected in multi-layered ultrathin films on further research [3,22]. In certain ferromagnetic material system with extremely low symmetry of the atomic arrangement and strong spin–orbit coupling, skyrmions can be formed and stabilized by the Dzyaloshinskii-Moriya interaction (DMI) [10,14,27], which originates from the broken or lack of inversion symmetry.

For the skyrmion-based STNO in the nanodisk with uniform DMI, the DMI is induced at the interface between the FM layer and heavy-metal (HM) layer. When a positive vertical spin current is applied on the nanodisk, a skyrmion moves in a straight-line trajectory towards the center, whereas skyrmion terminates at the edge of the nanodisk when an negative vertical spin current is applied [28,29]. Therefore, it is essential to design a unique physical model to induce regular motion of skyrmions to improve the performance of STNO.

In this work, we propose and design a layered structure with FM

* Corresponding authors.
E-mail addresses: ppong@eee.hku.hk (P.W.T. Pong), zhouyan@cuhk.edu.cn (Y. Zhou).

https://doi.org/10.1016/j.jmmm.2019.165912
Received 28 June 2019; Received in revised form 12 September 2019; Accepted 27 September 2019
Available online 01 October 2019
0304-8853/ © 2019 Elsevier B.V. All rights reserved.

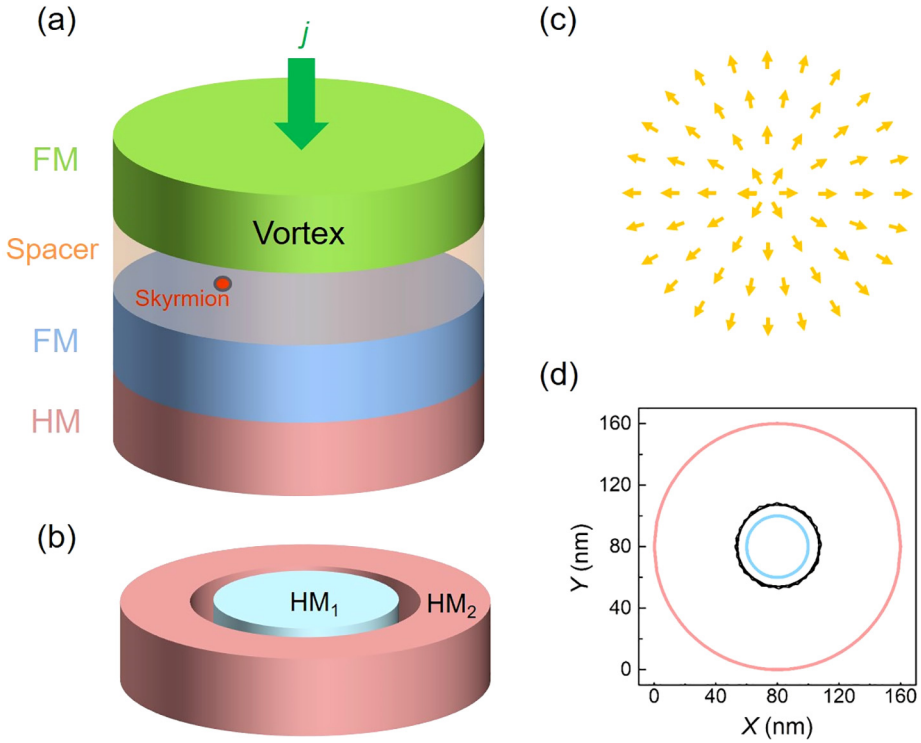

Fig. 1. (a) The simulated model of a skyrmion-based nano-oscillator. The top FM layer with a magnetic vortex configuration is used to generate the spin-polarized current with a vortex-like polarization. Such a spin-polarized current applies spin torques to the local magnetic moments of the bottom FM layer, and then the skyrmion in the bottom FM nanodisk moves in a circular motion. (b) The structure of one heavy metal embeds in another one, where the radiuses of HM_1 and HM_2 are 10 nm and 80 nm respectively. The inner (blue) and outer (pink) areas have different values of DMI. The skyrmion moves along the edge of the inner area. (c) The configuration of the polarization vector $\boldsymbol{m_p}$ of the spin current. (d) The trajectory of the skyrmion (black line). The blue and pink lines show the inner and outer nanodisk boundaries, respectively. (For interpretation of the references to colour in this figure legend, the reader is referred to the web version of this article.) (For interpretation of the references to colour in this figure legend, the reader is referred to the web version of this article.)

vortex layer/spacer layer/FM layer/HM layer, where the HM layer has one heavy metal embedded inside another one. The proposed heterostructure is aimed to maintain stable rotation of the skyrmion along a circular trajectory and create wide-ranging and steady frequency in STNO. The motion of a FM skyrmion in the bottom FM nanodisk is driven by the spin current with a vortex-like polarization and the top FM layer with a radial vortex spin configuration is used to generate the spin-polarized current with a vortex-like polarization. The spin-polarized current applies STT to the local magnetic moments of the bottom FM layer, and then the skyrmion in the bottom FM nanodisk moves in a circular motion.

2. Modelling and simulation details

The magnetization dynamics in the FM layer with skyrmions is described by the Landau-Lifshitz-Gilbert (LLG) equation, which is given as [16,25,26,30]

$$\frac{d\boldsymbol{m}}{dt} = -|\gamma|\,\boldsymbol{m}\times\boldsymbol{H}_{eff} + \alpha\left(\boldsymbol{m}\times\frac{d\boldsymbol{m}}{dt}\right) + |\gamma|\,\beta\,\epsilon\,\boldsymbol{m}\times(\boldsymbol{m}_p\times\boldsymbol{m}) - |\gamma|\,\beta\,\epsilon'\,\boldsymbol{m}\times\boldsymbol{m}_p \quad (1)$$

where $\boldsymbol{m}$ represents the reduced magnetization, M/M_S. γ and α are the gyromagnetic ratio and Gilbert damping constant, respectively. $\beta = \left|\frac{\hbar}{\mu_0 e}\right|\frac{j}{t_z M_S}$ where e is the electron charge in C, j is current density in A/m^2, t_z is the free layer thickness in meters, and M_S is the saturation magnetization in A/m. $\varepsilon = \frac{P\Lambda^2}{\Lambda^2+1+(\Lambda^2-1)(\boldsymbol{m}\cdot\boldsymbol{m_p})}$, as the prime STT term, P is the spin polarization rate and Lambda $\Lambda = 2$. $\boldsymbol{m_p}$ stands for the (unit) electron polarization direction, while ϵ' is related to secondary STT term.

On the other hand, the center-of-mass dynamics of a magnetic skyrmion can be described by the Thiele equation [15,31–33], derived as follows [18]

$$\boldsymbol{G}\times\boldsymbol{v} + \boldsymbol{F}_\alpha + \boldsymbol{F}_j + \boldsymbol{F}_b = 0 \quad (2)$$

where the first term is the Magnus force with the velocity of skyrmion and gyrovector $\boldsymbol{G} = 4\pi Q\mu_0 M_s t_z/\gamma\boldsymbol{e}_z$. The skyrmion number $Q = -\frac{1}{4\pi}\int dxdy\,[\boldsymbol{m}\cdot(\delta_x\boldsymbol{m}\times\delta_y\boldsymbol{m})]$ is equal to ± 1 for an isolated FM skyrmion, the vaccum permeability constant is μ_0, the free layer thickness is t_z and the gyromagnetic ratio is γ. The second term $\boldsymbol{F}_\alpha = =-\alpha\mu_0\boldsymbol{M}_s t_z\boldsymbol{v}\cdot\boldsymbol{d}/\gamma$ describes the dissipative force, with the damping α, the velocity $\boldsymbol{v}$ and the dis sipative tensor $\boldsymbol{d} = \begin{pmatrix} d & 0 \\ 0 & d \end{pmatrix}$, where $d = \int dxdy\delta_x\boldsymbol{m}\cdot\delta_x\boldsymbol{m}$. The third term $\boldsymbol{F}_j$ represents the current-induced driving force, which can be decomposed into two orthogonal directions ($\boldsymbol{e}_r$, the radial direction and $\boldsymbol{e}_t$, the tangential direction are both based on the symmetry of the nanodisk), i.e., $\boldsymbol{F}_j = F_{jt}\boldsymbol{e}_t + F_{jr}\boldsymbol{e}_r$ and $F_{ji} = -\mu_0 B_j M_s t_z\int dxdy\,[(\boldsymbol{m}\times\boldsymbol{p})\cdot\delta_i\boldsymbol{m}]$, where B_j means the applied vertical current density, which is defined as $j\hbar P/2\mu_0 eM_s t_z$ with the Planck constant $\hbar$, the spin polarization rate P and the elementary charge e. The last term F_b stands for the boundary-induced force, which $\boldsymbol{F}_b = -\nabla U$ with the potential energy U.

The Thiele equation for FM skyrmions can be decomposed into two orthogonal parts (radial and tangential directions) [34,35]. Therefore, Eq. (2) can be split as mentioned below [18]

$$v_t\boldsymbol{G}\times\boldsymbol{e}_t - F_b\boldsymbol{e}_r = 0 \quad (3)$$

$$F_\alpha\boldsymbol{e}_t + F_{jt}\boldsymbol{e}_t = 0 \quad (4)$$

From the above two equations, it is evident that the steady circular motion of a FM skyrmion within a nanodisk requires the boundary force to balance out the Magnus force.[27,36–41] However, both the boundary-induced force and Magnus force are pointing along the line going through the center of the nanodisk when j is positive, so that the FM skyrmion will move toward the nanodisk center eventually. For the negative current, although the Magnus force is pointing toward the edge of the nanodisk, the boundary-induced force is not strong enough to counterbalance the Magnus force, resulting in the destruction of the FM skyrmion at the nanodisk edge. Therefore, we create a composite force induced by using different values of DMI, as shown in Fig. 1. For the heavy metal layer, we adopt a core–shell structure which can be fabricated using advanced nanofabrication techniques [42]. Because the embedded heavy metal adopts different metal material with the

surrounded one, the DMI constant for the inner region is assumed to be smaller than that for the outer region. By adopting reasonable ranges of DMI in both inner and outer circular regions, the stable current-driven circular motion of a skyrmion on the FM nanodisk can be obtained, as shown in Fig. 1d.

In this work, all micromagnetic simulations are performed by using the Object Oriented Micromagnetic Framework (OOMMF) [43] with additional extension module employed to consider the DMI [44]. The time-dependent magnetization dynamics is governed by the LLG equation including both antidamping-like and field-like STTs [see Eq. (1)]. The standard magnetic parameters are adopted as [45]: saturation magnetization $M_S = 580 \times 10^3$ A/m, anisotropy coefficient $K_u = 0.8 \times 10^6$ J/m^3, exchange coefficient $A = 15.0 \times 10^{-12}$ J/m, Gyromagnetic ratio γ is -2.211×10^5 m/(A·s). DMI constants for the inner region $D_1 = 1.0$ mJ/m^2 and for the outer region $D_2 = 4.0$ mJ/m^2, current density $j = 2 \times 10^{11}$A/m^2, Gilbert damping coefficient $\alpha = 0.5$, nanodisk radius for the inner region $r = 10$ nm and for the outer region $R = 80$ nm unless otherwise specified. The FM layer thickness is set as 0.5 nm and the discretization cell size is set as $1 \times 1 \times 0.5$ nm^3. The configuration of the polarization vector $\boldsymbol{m_p}$ of the spin current is as shown in Fig. 1c. Initially, the skyrmion is located at the left side, where is the central point between the edge of the inner heavy metal (HM_1) and outer heavy metal (HM_2). Then, the system is relaxed over 2 ns before applying the driving current. The driving spin current is applied for 5 ns, within which the stable motion of skyrmion can be reached.

3. Results and discussion

The frequency of STNO can be significantly influenced under various current densities. Fig. 2(a) illustrates the periodic changes of the in-plane magnetization component (M_x) driven by the spin current for different current densities, which indicates that the frequency of STNO increases within increasing current density. The effect of current density on the frequency of oscillator is given in Fig. 2. It can be seen that the frequency of STNO is proportional to the current density for various D_1 and D_2. In addition, when the DMI strength rises at either inner or outer area, the frequency of STNO goes up as well. It should be mentioned that the injected current density should be controlled within a reasonable range since the skyrmion could be deformed and then destructed when the current density is larger than certain threshold. For example, when $D_1 = 1.0$ mJ/m^2 and $D_2 = 4.5$ mJ/m^2, the skyrmion will be destructed if the current density is larger than 3×10^{11}A/m^2. For the case of $D_1 = 1.0$ mJ/m^2 and $D_2 = 4.0$ mJ/m^2, the current density can be increased up to $j = 8 \times 10^{11}$A/m^2. As a result, the frequency of the circular motion of the skyrmion can reach 3.43 GHz.

As shown in Fig. 1b, the DMI constants (D_1, D_2) can also affect the performance of STNO in a reasonable range. The frequencies of STNO as functions of D_1, D_2, and ΔD are shown in Fig. 3. The increase in both D_1 and D_2 will lead to a rise in the performance of STNO, which is indicated by the increase of the oscillator frequency. By comparing the variation in DMI strengths from Fig. 3(a) and (b), it is noted that the effect of D_2 is more obvious than D_1 for a given change of DMI constant. The motion of skyrmion occurs in the outer region HM_2. And, the increase of D_2 results in the expansion of the skyrmion, leading to the increases of skyrmion velocity. As a result, the frequency increases with D_2. When D_1 increases, the expansion of the skyrmion leads to the faster movement of the skyrmion. Hence, the frequency increases with D_1. It should be mentioned that D_2 needs to be larger than D_1. When D_1 and D_2 are close, the energy barrier between HM_1 and HM_2 is so weak that the skyrmion will move to the center of the disk. Also, D_2 have reasonable ranges since the skyrmion cannot be stable when D_2 is too small or too large. We also show the effect ΔD, i.e., D_2-D_1, on the frequency as shown in Fig. 3(c) and (d). On one hand, the frequency is proportional to the difference ΔD when D_2 varies with a fixed D_1. On the other hand, the frequency is inversely proportional to the difference ΔD when D_1 varies with a fixed D_2.

The dependences of frequency and velocity on the damping constant α and the nanodisk geometries are shown in Fig. 4. In order to study the relation among the nanodisk radius, skyrmion velocity and oscillator frequency, the simulation is done by fixing $r = 10$ nm when R is varied, and $R = 80$ nm when r is changed. It can be seen from Fig. 4(a)–(d) that when both R and r are reduced, the frequency will increase. However, the velocity shows a linear proportional relation with radiuses in both inner and outer areas. The damping constant α has a negative impact on the performance of oscillator. It can be seen from Fig. 4(e) that a small damping α is beneficial to obtaining a high frequency. Fig. 4(f) indicates that the skyrmion velocity depends on α since v_t is inversely proportional to damping constantα. By observing the changes of magnetization moment, we can control each variable in a reasonable range so that the skyrmion cannot be destroyed or deformed in that condition. The maximum value of the oscillator frequency can be obtained as 3.43 GHz.

As a difference between that reported in Ref. 4 and our method, we can see that if the uniform DMI is adopted the skyrmion may move along the edge of the disk as a result of the competition between the repulsive force from the edge and the driving force from the spin-polarized current. In our work, as the inner and outer areas of the FM have different values of DMI, the skyrmion driven by the spin-polarized current with a vortex-like polarization could move along the outer edge of the area with smaller DMI. The radius of the circular motion is very small, which is helpful to obtain a higher frequency of STNO.

The STNO is frequently used as a microwave signal generator, where a microwave signal is generated by the precession of uniform magnetization or gyrotropic motion of a magnetic vortex. The most significant implementation of this working principle in STNOs is in the maximum and tuning range of oscillating frequency. In a system with the uniform DMI, it can be explained by splitting the Thiele equation that both the boundary-induced force and Magnus force are generated toward the center of the nanodisk when the current is positive or the boundary-induced force is not strong enough to offset the Magnus force for the negative current applied. That is to say, the boundary-induced force may not be strong enough to overcome the Magnus effect. This

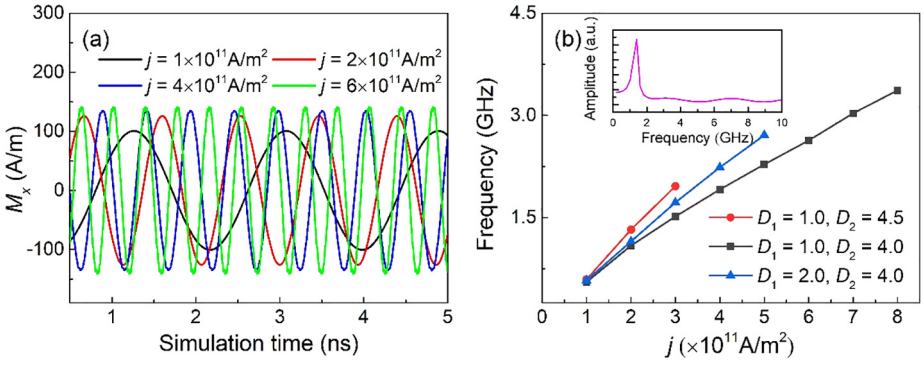

Fig. 2. The effect of current densities on the oscillation frequency. (a) The in-plane magnetization component (M_x) oscillates periodically with applying different current densities, indicating the circular motion of the skyrmion. (b) The frequency of the circular motion of the skyrmion as a function of the current density for various D_1 and D_2. The inset in (b) is the FFT power as a function of frequency with $j = 2 \times 10^{11}$ A/m^{-2}.

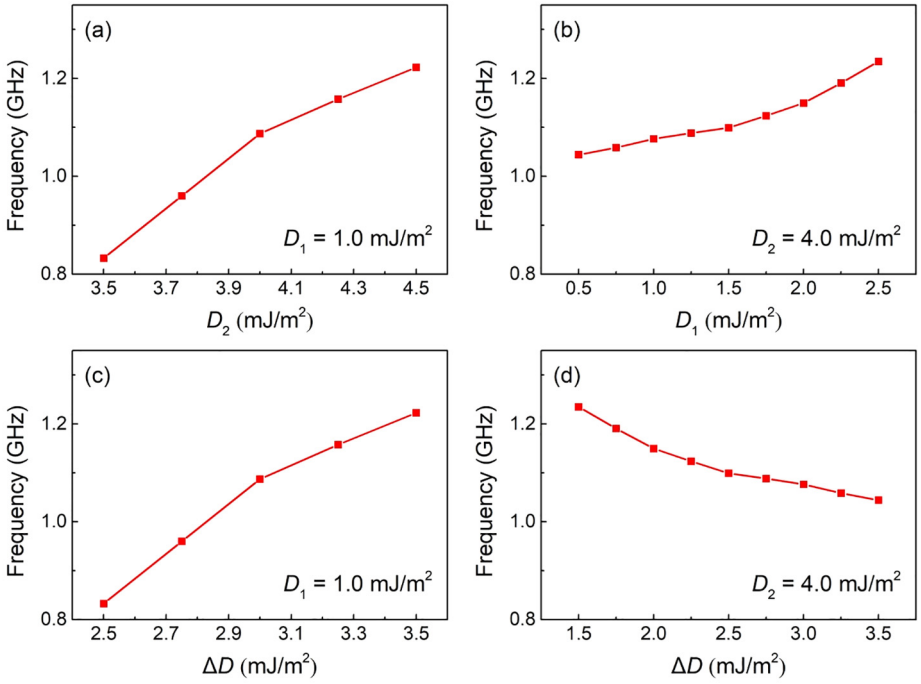

Fig. 3. The effect of DMI values on oscillation frequency. The current density is fixed at 2×10^{11}A/m^2 and nanodisk radiuses are fixed at $r = 10$ nm and $R = 80$ nm. (a) The frequency of skyrmion motion as a function of D_2 at a fixed $D_1 = 1.0$ mJ/m^2. (b) The frequency of skyrmion motion as a function of D_1 at a fixed $D_2 = 4.0$ mJ/m^2. (c)-(d) The frequency of skyrmion motion as a function of ΔD at a fixed $D_1 = 1.0$ mJ/m^2 (c) and $D_2 = 4.0$ mJ/m^2 (d). $\Delta D = D_2 - D_1$.

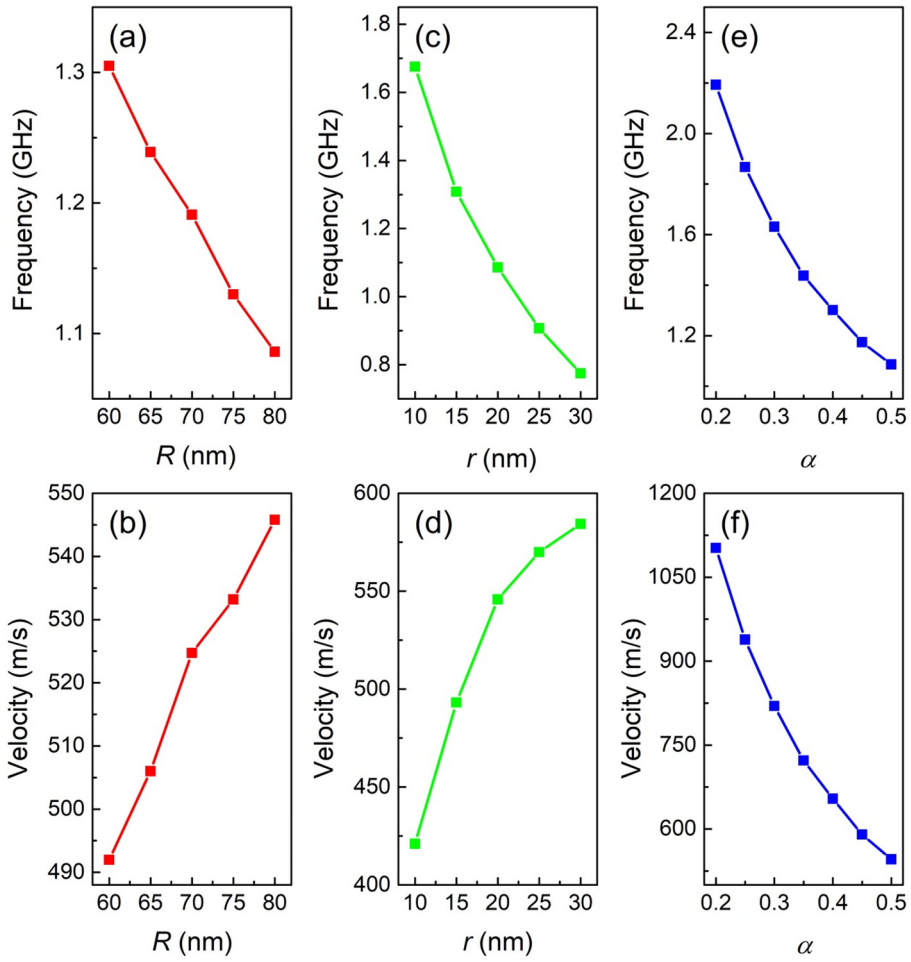

Fig. 4. The effect of nanodisk radiuses and damping constant on frequency of the oscillation and skyrmion velocity. The current density is fixed at 2×10^{11}A/m^2 and DMI constants are fixed at $D_1 = 1.0$ mJ/m^2 and $D_2 = 4.0$ mJ/m^2. (a)-(b) The frequency (a) and the velocity (b) of skyrmion motion as functions of R with a fixed r of 10 nm. (c)-(d) The frequency (c) and the velocity (d) of skyrmion motion as functions of r with a fixed R of 80 nm. (e)-(f) The frequency (e) and the velocity (f) of skyrmion motion as functions of the damping constant.

could lead to the motion of skyrmion towards the center of the nanodisk as well as the destruction of the FM skyrmion at the nanodisk edge. By using the proposed FM vortex layer / spacer layer / FM layer / HM layer model, the composite force from Magnus force and the boundary-induced force that acts as a centripetal force for the circular motion of skyrmion can be generated, similar to the case reported in a recent work in antiferromagnetic systems. On the basis of appropriate parameters, the STNO can thus be developed to meet more custom needs and possesses better performance.

4. Conclusion

In conclusion, a FM vortex layer/spacer layer/FM layer/HM layer model has been designed, which is used as a STNO based on FM skyrmions. The aim is to create a composite force from the Magnus force and boundary-induced force, inducing by two values of DMI, which can serve as the centripetal force to maintain stable circular motion of skyrmions. The dependence of the frequency of oscillator on magnetic parameters, driving current density, diameter of nanodisk are investigated and their optimal values are found. The numerical simulations show that the frequency ascends with an increase in both the current density and DMI values, and its maximum value is obtained as 3.43 GHz. The influences of changes in DMI in the outer area, D_2, is greater than that in the inner area, D_1. The effects of both radiuses will increase the skyrmion velocity, while decrease the frequency of the oscillator. Reducing the damping constant α will promote the motion of skyrmion and increase the frequency. However, it is noted that the range of α should be controlled since the skyrmion will be distorted significantly when the damping constant is smaller than 0.2. Our results provide an effective route to modulate the frequency in a wide range of future applications of FM skyrmion-based nano-oscillators.

Acknowledgements

P.W.T.P. acknowledges the support from the Seed Funding Program for Basic Research, Seed Funding Program for Applied Research and Small Project Funding Program from the University of Hong Kong, ITF Tier 3 funding (ITS/203/14, ITS/104/13, ITS/214/14), RGC-GRF grant (HKU 17210014, HKU 17204617), and University Grants Committee of Hong Kong (Contract No. AoE/P-04/08). X.Z. acknowledges the support by the Presidential Postdoctoral Fellowship of The Chinese University of Hong Kong, Shenzhen (CUHKSZ). Y.Z. acknowledges the support by the President's Fund of CUHKSZ, Longgang Key Laboratory of Applied Spintronics, National Natural Science Foundation of China (Grant Nos. 11974298 and 61961136006), Shenzhen Fundamental Research Fund (Grant No. JCYJ20170410171958839), and Shenzhen Peacock Group Plan (Grant No. KQTD20180413181702403).

References

[1] X. Jing, H. Zong-Yi, S. Yi-Fan, J. Wen-Jing, L. Liu-Rong, Z. Xi-Chao, L. Xiao-Xi, Z. Yan, Overview of magnetic skyrmion-based devices and applications, Acta. Phys. Sin. 67 (2018).
[2] G. Finocchio, F. Büttner, R. Tomasello, M. Carpentieri, M. Kläui, Magnetic skyrmions: from fundamental to applications, J. Phys. D: Appl. Phys. 49 (2016) 423001.
[3] A. Fert, N. Reyren, V. Cros, Magnetic skyrmions: advances in physics and potential applications, Nat. Rev. Mater. 2 (2017) 17031.
[4] F. Garcia-Sanchez, J. Sampaio, N. Reyren, V. Cros, J. Kim, A skyrmion-based spin-torque nano-oscillator, New J. Phys. 18 (2016) 075011.
[5] W. Kang, Y. Huang, X. Zhang, Y. Zhou, W. Zhao, Skyrmion-electronics: An overview and outlook, Proc. IEEE. 104 (2016) 2040.
[6] S.-Z. Lin, C. Reichhardt, C.D. Batista, A. Saxena, Particle model for skyrmions in metallic chiral magnets: Dynamics, pinning, and creep, Phys. Rev. B 87 (2013) 214419.
[7] C. Reichhardt, D. Ray, C.J.O. Reichhardt, Collective transport properties of driven skyrmions with random disorder, Phys. Rev. Lett. 114 (2015) 217202.
[8] N. Ran, G. Zhao, H. Tang, L. Shen, P. Lai, J. Xia, X. Zhang, Y. Zhou, The influence of the edge effect on the skyrmion generation in a magnetic nanotrack, AIP Adv. 7 (2017) 025105.
[9] P. Lai, G. Zhao, H. Tang, N. Ran, S. Wu, J. Xia, X. Zhang, Y. Zhou, An Improved Racetrack Structure for Transporting a Skyrmion, Sci. Rep. 7 (2017) 45330.
[10] X. Chen, W. Kang, D. Zhu, X. Zhang, N. Lei, Y. Zhang, Y. Zhou, W. Zhao, A compact skyrmionic leaky–integrate–fire spiking neuron device, Nanoscale 10 (2018) 6139.
[11] S. Bhatti, R. Sbiaa, A. Hirohata, H. Ohno, S. Fukami, S. Piramanayagam, Spintronics based random access memory: a review, Mater. Today 20 (2017) 530.
[12] C. Chui, Y. Zhou, Skyrmion stability in nanocontact spin-transfer oscillators, AIP Adv. 5 (2015) 097126.
[13] S. Zhang, J. Wang, Q. Zheng, Q. Zhu, X. Liu, S. Chen, C. Jin, Q. Liu, C. Jia, D. Xue, Current-induced magnetic skyrmions oscillator, New J. Phys. 17 (2015) 023061.
[14] Z. He, S. Angizi, D. Fan, Current-induced dynamics of multiple skyrmions with domain-wall pair and skyrmion-based majority gate design, IEEE. Magn. Lett. 8 (2017) 1.
[15] J. Xia, Y. Huang, X. Zhang, W. Kang, C. Zheng, X. Liu, W. Zhao, Y. Zhou, A microwave field-driven transistor-like skyrmionic device with the microwave current-assisted skyrmion creation, J. Appl. Phys. 122 (2017) 153901.
[16] M. Mochizuki, S. Seki, Dynamical magnetoelectric phenomena of multiferroic skyrmions, J. Phys. Condens. Matter. 27 (2015) 503001.
[17] M. Mochizuki, Spin-wave modes and their intense excitation effects in skyrmion crystals, Phys. Rev. Lett. 108 (2012) 017601.
[18] L. Shen, J. Xia, G. Zhao, X. Zhang, M. Ezawa, O.A. Tretiakov, X. Liu, Y.J.A.P.L. Zhou, Spin torque nano-oscillators based on antiferromagnetic skyrmions, Appl. Phys. Lett. 114 (2019) 042402.
[19] X. Zhang, G. Zhao, H. Fangohr, J.P. Liu, W. Xia, J. Xia, F.J. Morvan, Skyrmion-skyrmion and skyrmion-edge repulsions in skyrmion-based racetrack memory, Sci. Rep. 5 (2015) 7643.
[20] W. Kang, C. Zheng, Y. Huang, X. Zhang, W. Lv, Y. Zhou, W. Zhao, Compact modeling and evaluation of magnetic skyrmion-based racetrack memory, IEEE T Electron Dev. 64 (2017) 1060.
[21] B. Krüger, A. Drews, M. Bolte, U. Merkt, D. Pfannkuche, G. Meier, Vortices and antivortices as harmonic oscillators, J. Appl. Phys. 103 (2008) 07A501.
[22] R. Nepal, U. Güngördü, A.A. Kovalev, Magnetic skyrmion bubble motion driven by surface acoustic waves, Appl. Phys. Lett. 112 (2018) 112404.
[23] X. Zhang, Y. Zhou, M. Ezawa, Magnetic bilayer-skyrmions without skyrmion Hall effect, Nat. Commun. 7 (2016) 10293.
[24] J. Smet, R. Deutschmann, F. Ertl, W. Wegscheider, G. Abstreiter, K. Von Klitzing, Gate-voltage control of spin interactions between electrons and nuclei in a semiconductor, Nature 415 (2002) 281.
[25] M.R. Pufall, W.H. Rippard, S. Kaka, T.J. Silva, S.E. Russek, Frequency modulation of spin-transfer oscillators, Appl. Phys. Lett. 86 (2005) 082506.
[26] W. Jiang, J. Xia, X. Zhang, Y. Song, C. Ma, H. Fangohr, G. Zhao, X. Liu, W. Zhao, Y. Zhou, Dynamics of magnetic skyrmion clusters driven by spin-polarized current with a spatially varied polarization, IEEE. Magn. Lett. 9 (2018) 1.
[27] J. Xia, X. Zhang, M. Yan, W. Zhao, Y. Zhou, Spin-Cherenkov effect in a magnetic nanostrip with interfacial Dzyaloshinskii-Moriya interaction, Sci. Rep. 6 (2016) 25189.
[28] X. Zhang, Y. Zhou, M. Ezawa, Antiferromagnetic skyrmion: stability, creation and manipulation, Sci. Rep. 6 (2016) 24795.
[29] J. Barker, O.A. Tretiakov, Static and dynamical properties of antiferromagnetic skyrmions in the presence of applied current and temperature, Phys. Rev. Lett. 116 (2016) 147203.
[30] Y. Zhou, E. Iacocca, A.A. Awad, R.K. Dumas, F. Zhang, H.B. Braun, J. Åkerman, Dynamically stabilized magnetic skyrmions, Nat. Commun. 6 (2015) 8193.
[31] X. Zhang, J. Müller, J. Xia, M. Garst, X. Liu, Y. Zhou, Motion of skyrmions in nanowires driven by magnonic momentum-transfer forces, New J. Phys. 19 (2017) 065001.
[32] N. Kanazawa, S. Seki, Y. Tokura, Noncentrosymmetric magnets hosting magnetic skyrmions, Adv. Mater. 29 (2017) 1603227.
[33] J. Iwasaki, M. Mochizuki, N. Nagaosa, Universal current-velocity relation of skyrmion motion in chiral magnets, Nat. Commun. 4 (2013) 1463.
[34] B. Piette, R. Ward, Planar Skyrmions: vibrational modes and dynamics, Physica. D. 201 (2005) 45.
[35] Y. Zhou, M. Ezawa, A reversible conversion between a skyrmion and a domain-wall pair in a junction geometry, Nat. Commun. 5 (2014) 4652.
[36] G. Yin, Y. Li, L. Kong, R.K. Lake, C.-L. Chien, J. Zang, Topological charge analysis of ultrafast single skyrmion creation, Phys. Rev. B. 93 (2016) 174403.
[37] C. Schütte, J. Iwasaki, A. Rosch, N. Nagaosa, Inertia, diffusion, and dynamics of a driven skyrmion, Phys. Rev. B 90 (2014) 174434.
[38] W. Jiang, X. Zhang, G. Yu, W. Zhang, X. Wang, M.B. Jungfleisch, J.E. Pearson, X. Cheng, O. Heinonen, K.L. Wang, Direct observation of the skyrmion Hall effect, Nat. Phys. 13 (2017) 162.
[39] S. Woo, K.M. Song, X. Zhang, Y. Zhou, M. Ezawa, X. Liu, S. Finizio, J. Raabe, N.J. Lee, S.-I. Kim, Current-driven dynamics and inhibition of the skyrmion Hall effect of ferrimagnetic skyrmions in GdFeCo films, Nat. Commun. 9 (2018) 959.
[40] C. Ma, X. Zhang, J. Xia, M. Ezawa, W. Jiang, T. Ono, S. Piramanayagam, A. Morisako, Y. Zhou, X. Liu, Electric field-induced creation and directional motion of domain walls and skyrmion bubbles, Nano Lett. 19 (2018) 353.
[41] X. Zhang, M. Ezawa, Y. Zhou, Magnetic skyrmion logic gates: conversion, duplication and merging of skyrmions, Sci. Rep. 5 (2015) 9400.
[42] G. Duerr, M. Madami, S. Neusser, S. Tacchi, G. Gubbiotti, G. Carlotti, D. Grundler, Spatial control of spin-wave modes in $Ni_{80}Fe_{20}$ antidot lattices by embedded Co nanodisks, Appl. Phys. Lett. 99 (2011) 202502.
[43] J.P. Adam, S. Rohart, J.P. Jamet, J. Ferré, A. Mougin, R. Weil, H. Bernas, G. Faini, Magnetization reversal by confined droplet growth in soft/hard hybrid nanodisks with perpendicular anisotropy, Physical Review B 85 (2012) 214417.
[44] S. Rohart, A. Thiaville, Skyrmion confinement in ultrathin film nanostructures in the presence of Dzyaloshinskii-Moriya interaction, Phys. Rev. B 88 (2013) 184422.
[45] X. Zhang, M. Ezawa, D. Xiao, G. Zhao, Y. Liu, Y. Zhou, All-magnetic control of skyrmions in nanowires by a spin wave, Nanotechnology 26 (2015) 225701.